Binding and Activation of Thiamin Diphosphate in Acetohydroxyacid Synthase†

Ahuva Bar-Ilan,‡ Vitaly Balan,‡ Kai Tittmann,§ Ralph Golbik,§ Maria Vyazmensky,‡ Gerhard Hübner,§ Ze'ev Barak,‡ and David M. Chipman*,‡

Department of Life Sciences, Ben-Gurion University of the Negev, P.O.B. 653, Beer-Sheva 84105, Israel, and Department of Biochemistry, Martin-Luther-University Halle-Wittenberg, Kurt-Mothes-Strasse 3, D-06099 Halle, Germany

Received March 6, 2001; Revised Manuscript Received August 1, 2001

ABSTRACT: Acetohydroxyacid synthases (AHASs) are biosynthetic thiamin diphosphate- (ThDP) and FAD-dependent enzymes. They are homologous to pyruvate oxidase and other members of a family of ThDP-dependent enzymes which catalyze reactions in which the first step is decarboxylation of a 2-ketoacid. AHAS catalyzes the condensation of the 2-carbon moiety, derived from the decarboxylation of pyruvate, with a second 2-ketoacid, to form acetolactate or acetohydroxybutyrate. A structural model for AHAS isozyme II (AHAS II) from *Escherichia coli* has been constructed on the basis of its homology with pyruvate oxidase from *Lactobacillus plantarum* (*Lp*POX). We describe here experiments which further test the model, and test whether the binding and activation of ThDP in AHAS involve the same structural elements and mechanism identified for homologous enzymes. Interaction of a conserved glutamate with the N1′ of the ThDP aminopyrimidine moiety is involved in activation of the cofactor for proton exchange in several ThDP-dependent enzymes. In accord with this, the analogue *N*3′-pyridyl thiamin diphosphate does not support AHAS activity. Mutagenesis of Glu47, the putative conserved glutamate, decreases the rate of proton exchange at C-2 of bound ThDP by nearly 2 orders of magnitude and decreases the turnover rate for the mutants by about 10-fold. Mutant E47A also has altered substrate specificity, pH dependence, and other changes in properties. Mutagenesis of Asp428, presumed on the basis of the model to be the crucial carboxylate ligand to Mg^{2+} in the "ThDP motif", leads to a decrease in the affinity of AHAS II for Mg^{2+}. While mutant D428N shows ThDP affinity close to that of the wild-type on saturation with Mg^{2+}, D428E has a decreased affinity for ThDP. These mutations also lead to dependence of the enzyme on K^{+}. These experiments demonstrate that AHAS binds and activates ThDP in the same way as do pyruvate decarboxylase, transketolase, and other ThDP-dependent enzymes. The biosynthetic activity of AHAS also involves many other factors beyond the binding and deprotonation of ThDP; changes in the ligands to ThDP can have interesting and unexpected effects on the reaction.

In the past few years, a clear picture has emerged for the mechanism of enzymatic activation of thiamin diphosphate (ThDP).[1] All enzymes which utilize ThDP as coenzyme appear to have several common, conserved elements in their ThDP-binding sites (*1*−*8*). The diphosphate group of ThDP is bound to one domain of the protein via a chelated divalent metal ion (usually Mg^{2+}); the metal-binding site of the protein involves three ligand atoms from a "thiamin diphosphate motif" of conserved sequence (*9*). A highly conserved glutamic acid in another domain is within hydrogen-bonding distance of N1′ of the pyrimidine moiety of ThDP. ThDP adopts a "V-conformation" in the active site, which places the pyrimidine N4′ in a position to remove the thiazolium C2 proton (Figure 1, top). It has been shown experimentally for several enzymes that the conserved glutamate−aminopyrimidine interaction is essential for deprotonation of C2 and thus for activation of the coenzyme (*10*−*14*). In many of the ThDP-dependent enzymes, a symmetric dimer of identical subunits binds two ThDP molecules, each lying between the pyrimidine-binding domain of one subunit and diphosphate-binding domain of the other (*3*−*6*, *15*).

Acetohydroxyacid synthases (AHASs) are a group of biosynthetic ThDP- and FAD-dependent enzymes which share significant sequence homology with pyruvate oxidase and other members of a family of ThDP-dependent enzymes which catalyze reactions in which the common first step is decarboxylation of pyruvate (or a similar 2-ketoacid) (*16*). There are no experimental three-dimensional structures available for any AHAS, but structural models for AHAS isozyme II (AHAS II) from *Escherichia coli* (*17*) and AHAS from *Arabidopsis thaliana* (*18*) have been constructed on the basis of their homologies with pyruvate oxidase from *Lactobacillus plantarum* (*Lp*POX). Although the sequence homology between AHASs and pyruvate oxidases appears

† This research was begun with funds from Grant 93-00233 (to D.M.C., Z.B., and John V. Schloss) from the United States−Israel Binational Science Foundation and continued with funding from a Seed Grant from the Vice-President for Research and Development of Ben-Gurion University. D.M.C. is the incumbent of The Lily and Sidney Oelbaum Chair in Applied Biochemistry.

* Correspondence should be addressed to this author. Tel: [+972]-8-647 2646. Fax: [+972]-8-647 2890. Email: chipman@bgumail.bgu.ac.il.

‡ Ben-Gurion University of the Negev.

§ Martin-Luther-University Halle-Wittenberg.

[1] Abbreviations: AHAS, acetohydroxyacid synthase; *Lp*POX, pyruvate oxidase from *Lactobacillus plantarum*; N3ThDP, *N*3′-pyridyl thiamin diphosphate; ThDP, thiamin diphosphate; HEThDP, hydroxyethylthiamin diphosphate; SMM, sulfometuron methyl; 2KB, 2-ketobutyrate.

10.1021/bi0104524 CCC: $20.00
Published on Web 09/07/2001

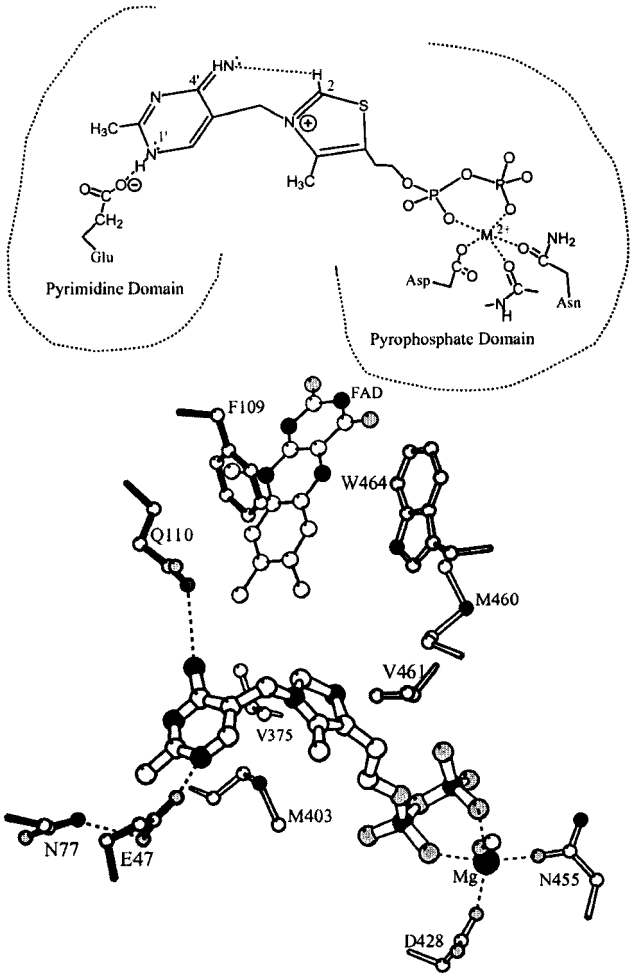

FIGURE 1: (Top) Schematic representation of a canonical ThDP-binding site, with the conserved glutamate residue within H-bonding distance of the pyrimidine N1′, and the divalent metal complexed to the diphosphate, the conserved aspartate, and asparagine and a backbone oxygen. The pyrimidine- and diphosphate-binding subsites are parts of two different protein domains. In *Lp*POX and other proteins homologous in sequence to AHAS, the two domains are the first and third domains, respectively, in two identical polypeptides which form a symmetric dimer. (Bottom) The active site of AHAS II, from the homology model (*17*). ThDP is shown with thick bonds in the center of the figure. Protein side chains close to ThDP or to the likely position of bound substrates are shown, with residues from the first domain of one subunit in black and those from the third domain of the other subunit in white. Amino acids whose backbone atoms contribute polar interactions are not shown, to simplify the picture. The isoalloxazine moiety of FAD is also shown.

to be significant, and both classes of enzyme require ThDP, Mg^{2+}, and FAD for their activity, there are important differences between *Lp*POX and AHAS. AHAS is a biosynthetic enzyme and catalyzes the condensation of the 2-carbon moiety, derived from the decarboxylation of pyruvate, with the carbonyl carbon of a second 2-ketoacid, either pyruvate or 2-ketobutyrate, to form acetolactate or acetohydroxybutyrate, respectively (*19*, *20*). Bacterial AHASs are composed of catalytic subunits and small, regulatory subunits of unrelated structure, in an $\alpha_2\beta_2$ heterotetramer. *Lp*POX, like most other members of its family of homologous ThDP-dependent enzymes, is a homotetramer.

We describe here experiments designed to examine our model for the active site of AHAS II from *E. coli* (Figure 1, bottom) (*17*) and to test whether the binding and activation of ThDP in this enzyme indeed involve the same structural elements and mechanism identified for homologous enzymes. We have modified two residues in AHAS II by site-directed mutagenesis: Glu47 is the putative conserved glutamate whose interaction with the N1′ of the aminopyrimidine moiety is involved in activation of ThDP. Asp428 presumably provides the conserved aspartate (within the sequence GDG.... at the beginning of the "ThDP motif") which is a ligand for Mg^{2+}. Kinetic parameters, including the rate of proton exchange at C2 of bound ThDP, have been determined for the mutant enzymes. In addition to supporting our assumption that AHAS II and *Lp*POX are closely related in mechanism, our results cast light on aspects of the unique and specific condensation with a second 2-ketoacid, catalyzed by AHAS.

MATERIALS AND METHODS

Reagents. Sodium pyruvate, FAD, ThDP, and creatine were obtained from Sigma Chemical Co. (St. Louis, MO). 1-Naphthol was obtained from Carlo Erba Reagenti (Milano, Italy). Acid-washed activated charcoal was purchased from BDH (Poole, U.K.). ToyoPearl Phenyl 650 TSK was from Merck (Darmstadt, Germany). All other chemicals and reagents were of analytical grade and purchased from commercial sources. Sulfometuron methyl (SMM) was a gift of Dr. J. V. Schloss, then of E. I. DuPont and Co., Central R&D Department, Wilmington, DE. *N*3′-Pyridyl thiamin diphosphate (N3ThDP) was prepared as previously described (*21*). Restriction and modification enzymes were purchased from New England Biolabs (Beverly, MA) and MBI Fermentas (Amherst, NY).

Bacterial Strains and Plasmids. Escherichia coli XL-1-Blue strain (Stratagene Europe, Amsterdam) was used as the host bacteria in the process of construction of wild-type and mutated plasmids. Transformed *E. coli* BL21(DE3) strains (Novagene, Milwaukee, WI) were used for induced overexpression of the enzymes. The pRSET B plasmid (Invitrogen, Leek, The Netherlands) was used for constructing the pRGM expression vector. The plasmid pAH29 (*22*) containing the entire coding region of *E. coli* AHAS II (*ilvG2096* mutation) was a gift of G. W. Hatfield. Plasmid pET-GM (*23*) was a gift from R. G. Duggleby.

Construction of Plasmid pRGM. Standard procedures for manipulation of DNA were used (*24*). The plasmid pRGM, for induced overexpression of the AHAS II holoenzyme, was constructed by insertion of two fragments of *ilvGM* between the *Eco*RI and *Nde*I sites of the pRSET B plasmid. The first was a 737 bp *Nde*I−*Sph*I fragment that covers the 5′ end of *ilvG*, derived by digestion and purification of the PCR product amplified from pAH29 using primers 1 and 2 (Table 1). Primer 1 creates an *Nde*I site in the 5′ end of the fragment to allow insertion into the plasmid. The second fragment (1160 bp), that includes the remainder of *ilvGM*, was isolated by digestion of plasmid pET-GM with *Sph*I and *Eco*RI. Most of the regions amplified by PCR, including that taken from pET-GM (*23*), from the *Nsi*I site (95 bp downstream of the *ilvG* start codon) to the *Aat*II site (75 bp upstream of the *ilvM* stop codon), were then replaced with the fragment from the original *ilvGM* gene from plasmid pAH29 (*22*). The plasmid pRGM encodes a protein that is identical in sequence and activity to the original AHAS enzyme of *E. coli* *ilvG*2096 with no additions.

Table 1: Sequence of Primers Used in PCR Mutagenesis

	primer	sequence[a]
1	G-Nde-met[b]	5′ CGGGGAACTA***CA****TATG*AATGGCGCAC 3′
2	1415−1396[b]	5′ ATAGCGTCACCGGGATGGTC 3′
3	E47Qfor	5′ ATGCCGACAT**C**AGCAGGGTGCGG 3′
4	E47Qrev	5′ CCGCACCCTGC**T**GATGTCGGCAT 3′
5	E47Afor	5′ ATGCCGACAT**G**C**G**CAGGGTGCGG 3′
6	E47Arev	5′ CCGCACCCTG**C**G**C**ATGTCGGCAT 3′
7	BSph[c]	5′ CTGGGCATGCTGGGGATGCACGG 3′
8	d-primer[c]	5′ AACTTAAGGAAAACGCGAGTCCG 3′
9	D428Efor	5′ ATCTCCGGTGA**G**GGCTCTTTCAT 3′
10	D428Erev	5′ ATGAAAGAGCC**C**TCACCGGAGAT 3′
11	D428Nfor	5′ ATCTCCGGT**A**AC**G**GCTCTTTCAT 3′
12	D428Nrev	5′ ATGAAAGAGCCG**T**TACCGGAGAT 3′

[a] The relevant mutated triplet codons are underlined, and the altered bases are shown in boldface type. The bases creating the new *Nde*I site are indicated in italics in primer 1. [b] Primers used as the flanking primers in construction of pRGM and mutants at E47. [c] Primers used as the flanking primers in construction of mutants at D428.

Site-Directed Mutagenesis. Site-directed mutants were constructed by the overlap extension PCR method (*25*). This is a three-reaction procedure requiring two overlapping mutagenic primers and two flanking primers (Table 1). To construct the mutations at Asp428, the mutagenized PCR fragments were digested with *Kpn*I and *Mlu*I and ligated into the appropriately digested pRGM. For construction of the Glu47 mutants, the PCR fragment was digested with *Nde*I and *Sph*I to yield a 737 bp fragment. This fragment could not be directly ligated into pRGM, as the plasmid has two *Nde*I sites. Instead, the fragment was ligated with two separately derived fragments of pRGM, the 1160 bp *Sph*I−*Eco*RI fragment and the *Nde*I−*Eco*RI fragment. All mutations were confirmed by DNA sequence determination.

Growth and Induction of Bacterial Cells. For expression of AHAS II and its mutants, the plasmid pRGM and its derivatives were transformed into *E. coli* BL21(DE3). To avoid loss of plasmids, which occurs at stationary phase, transformed cultures were kept in the exponential phase. Thus, stock cultures were prepared from freshly transformed bacteria grown in LB medium at 37 °C with ampicillin (100 μg/mL) to an OD_{660} of ∼0.6 and the cells stored with 20% glycerol at −80 °C. For preparation of enzymes, stock cultures were diluted to OD_{660} 0.02−0.025 in LB medium containing 100 μg/mL ampicillin. The bacteria were then grown with shaking (200 rpm) at 37 °C in several 600 mL liquid cultures in 2 L flasks. Expression was induced in the cultures at OD_{660} 0.3−0.5 by adding 0.4 mM IPTG. The cells were harvested after 2−3 h and washed twice with 0.1 M Tris-HCl (pH 7.8), and intact cells were stored at −20 °C.

Purification of Enzymes. The purification of AHAS II could be simplified relative to that previously published for *Salmonella typhimurium* AHAS II (*26*) because the expression vector used here gave a high yield of the desired protein. Frozen cells of *E. coli* BL21(DE3)/pRGM were suspended (1 g wet cells to 10 mL) in buffer A (0.1 mM FAD, 1 mM DTT, 10 mM EDTA in 0.1 M Tris-HCl, pH 7.8) and disrupted by sonication at 0 °C (6 × 20 s with 40 s intervals, at maximum power with Heat System model XL2015 ultrasonic liquid processor). Debris was pelleted by centrifugation (27000*g*, 4 °C, 1 h). A solution of 2% protamine sulfate was slowly added to the supernatant with mixing at room temperature to a final ratio of 12 mg of protamine sulfate per 1 g of initial cells. The pellet was discarded by centrifugation (27000*g*, 4 °C, 20 min), and ammonium sulfate (20 g to each 100 mL) was slowly added to the supernatant. After incubation for 30 min at room temperature, the precipitate was collected by centrifugation as above. It was then dissolved in buffer A (half of initial volume). To this solution was slowly added with stirring an equal volume of 1.4 M ammonium sulfate in buffer A. Sediments were discarded by centrifugation for 20 min, and the soluble protein solution was loaded at a flow rate of 0.5 mL min^{-1} on a column (1 × 16 cm) containing 12 mL of ToyoPearl Phenyl 650 TSK. The loaded column was washed with 50 mL of buffer B (20 μM FAD, 1 mM DTT, 10 mM EDTA in 0.1 M Tris-HCl, pH 7.8), containing 0.7 M ammonium sulfate. This was followed by washing with 20 mL of buffer B containing 0.6 M ammonium sulfate. The column was further eluted at the loading flow rate with buffer C (20 μM FAD, 1 mM DTT, and 1 mM EDTA in 25 mM Tris-HCl, pH 7.8); the AHAS peak appeared at about 18 mL (1.5 volumes of the column). This protein was concentrated to 20−75 mg/mL by pressure dialysis using an Amicon PM10 membrane, or by dialysis against glycerol, and stored at −30 °C. During the purification, the protein and solutions were shielded from light to prevent loss of enzymatic activity, and all the steps after the ammonium sulfate precipitation were carried out at 4 °C.

The AHAS II mutants were purified by the same procedure used for the wild-type, with slight modifications. For example, the E47Q mutant was loaded on the hydrophobic column in buffer B containing only 0.58 M ammonium sulfate. In some cases, a Butyl 650 TSK column was used in place of the Phenyl column, with a starting ammonium sulfate concentration of 0.5 M.

Enzyme Assay. The AHAS catalytic activity was determined by the colorimetric method (*27*) at 37 °C. The activity is expressed in units (U) (1 U = 1 μmol of acetolactate formed min^{-1}). A 0.1 M potassium phosphate buffer, pH 7.6, containing 100 mM sodium pyruvate as substrate, was used for most assays. Tricine-KOH buffer (0.1 M) was used in studies of mutants at D428 to simplify the manipulation of Mg^{2+} concentrations. As mutants at E47 and D428 had decreased affinities for cofactors, experiments with these mutants were carried out in the presence of 500 μM ThDP, 200 μM FAD, and 10 mM $MgCl_2$, rather than the standard 100 μM ThDP, 75 μM FAD generally used (*27*). In every case, experiments were carried out in the same assay solution with a mutant and the wild-type protein in parallel; the wild-type protein was not affected by these changes in buffer and cofactor concentrations. The contribution of control, nonenzymatic synthesis of acetolactate or acetoin was insignificant. The possibility that other enzymes contribute to the observed synthesis rate for the mutants can be excluded by the high specificity observed in the competition assay (see below and Results).

K_m for pyruvate and $K_{0.5}$ for cofactors were determined by varying the concentration of the factor in question in the presence of saturating concentrations of all other factors. The substrate specificity for 2-ketobutyrate as second substrate, *R* (*28*), was determined by measuring acetohydroxybutyrate and acetolactate formation simultaneously in a competition experiment with 2-ketobutyrate and pyruvate, in the standard buffer (*20*). The results were fit with the program "SigmaPlot" to the simultaneous equations:

$$V_{AHB}/V_t = R[2KB]/([pyruvate] + R[2KB])$$

$$V_{AL}/V_t = [pyruvate]/([pyruvate] + R[2KB])$$

where [2KB] is the concentration of 2-ketobutyrate and V_{AHB}/V_t and V_{AL}/V_t are the observed rates of formation of acetohydroxybutyrate and acetolactate, relative to the sum of their rates (*20*).

The continuous assay of AHAS activity was carried out under the standard conditions, by following the disappearance of the absorbance of pyruvate at 333 nm (*26*), using a Beckmann DU640 spectrophotometer. The data were fit to the empirical equation: $OD = y_0 + (v/b)e^{-bt} - vt$, where v is the steady-state rate of disappearance of absorption and b is the first-order rate of approach to the steady-state.

Protein concentration was determined by the dye-binding method of Bradford (*29*), with bovine serum albumin as standard.

Stripping of FAD from AHAS. Determination of the apparent affinity of the enzyme for FAD required removal of the tightly bound cofactor with charcoal in high salt (*23*, *26*). The proteins were incubated with 5% activated charcoal and 1.6 M KCl in 25 mM Tris-HCl, pH 7.8, for 30 min on ice, and the charcoal was removed by centrifugation at 4 °C.

Mg^{2+} Dependence. Protein was prepared from the sonication step onward with EDTA. A sample at a concentration of about 1 mg/mL was incubated on ice for 5 min with 10 mM EDTA to remove any remaining bound magnesium. A 20 μL sample of this solution (diluted if necessary) was added to reaction mixtures (1 mL) containing varying amounts of $MgCl_2$ in 0.1 M Tricine-KOH buffer, pH 8.0. The free Mg^{2+} concentration was calculated from the total EDTA and Mg^{2+} in the reaction mixture, with the program MAX CHELATOR.v6.8 using the stability constants of Martell and Smith (*30*).

Determination of the Exchange Rate. The kinetics of H/D exchange of the C2−H of ThDP were measured by ^{1}H NMR (*13*). Immediately before the exchange experiments, enzymes were incubated with stoichiometric amounts of ThDP and FAD for 4−6 min at 37 °C in 0.1 M potassium phosphate buffer, pH 7.6, containing 5 mM Mg^{2+}. The exchange reactions were initiated by mixing equal volumes of enzyme and cofactors, or 1 mM ThDP alone, with D_2O in a quenched-flow apparatus (model RQF-3, Kin Tek Althouse, USA) at 37 °C. Reactions were stopped by addition of final concentrations of 0.1 M hydrochloric acid and 5% (w/v) trichloroacetic acid. Exchange times were varied between 5 and 2000 ms. Experiments for longer times were performed by manual mixing. After separation of the denatured protein by centrifugation, the ^{1}H NMR spectra of the supernatants containing ThDP and FAD, in a 5 mm NMR tube, were recorded on a Bruker ARX 500 MHz NMR spectrometer. The triplet signal of the α-CH_2 of ThDP at 3.36 ppm was used as a nonexchanging internal standard. We fixed this integral as 2 and determined the relative signal integral of the C2-proton at 9.68 ppm. To obtain the exchange rate, the relative decay in the integral intensity of the C2−H signal was fitted to a pseudo-first-order decay to a final value. The signals due to FAD do not interfere with the signals of the C2 proton or the α-CH_2 group of ThDP.

RESULTS

The high level of expression of *E. coli* AHAS II from the plasmid pRGM, under control of the T7 promoter, allowed us to simplify the purification procedure of Schloss et al. (*26*) to two steps. This plasmid is convenient for mutagenesis by the overlap extension PCR method (*25*), as it allows cassette replacement of mutated fragments in unique restriction sites. The specific activity of the pure wild-type enzyme was about 20 U mg^{-1}, similar to that previously reported (*23*, *26*). The host strain *E. coli* BL21(DE3) has endogenous AHAS activity, but this activity is negligible under our growth conditions because of repression of genomic AHAS activity by the branched-chain amino acids contained in the LB-rich medium. This endogenous expression leads to an AHAS activity in the crude extract of <0.004 U mg^{-1}, as compared to $\sim$4 U mg^{-1} in the crude extract after induction of expression from pRGM, and $\sim$0.2 U mg^{-1} after induction of expression from the plasmids encoding the relatively inactive mutants.

Role of the Aminopyrimidine Moiety of ThDP. The assumption, that the aminopyrimidine moiety of ThDP has the same crucial function in AHAS as has been demonstrated in pyruvate decarboxylase, pyruvate dehydrogenase, and transketolase (*10*), was investigated by the use of the analogue *N3′*-pyridyl-ThDP (N3ThDP), in which the N1′ atom of the cofactor is substituted by C−H. Wild-type AHAS II was depleted of ThDP by gel filtration through Sephadex G50. Without addition of ThDP, the depleted sample showed 1.1 ± 0.1% of the activity observed with 100 μM ThDP. Under standard conditions with 100 μM N3ThDP, the same sample gave 1.3 ± 0.2% of the activity with 100 μM ThDP. Thus, the analogue has no significant activity, and the maximum activity attributable to the analogue is less than 0.5% of that observed with the normal coenzyme.

As the interaction between N1′ of ThDP and the carboxylate of Glu47 would be expected to play a role in coenzyme binding (see below), it was important to demonstrate that N3ThDP is in fact bound to AHAS II under the conditions of the activity experiment. The association of N3ThDP with the enzyme was demonstrated by a continuous assay of pyruvate disappearance after addition of ThDP to AHAS II preincubated with substrate, FAD, and Mg^{2+} in the presence or absence of N3ThDP. A typical experiment is shown in Figure 2. From the first-order approach of the rate of pyruvate disappearance to steady-state (Figure 2A), the apparent rate of binding of ThDP to the enzyme to form the active holoenzyme can be estimated to be 1.0×10^4 M^{-1} s^{-1}. This rate is decreased to $(5 \pm 1) \times 10^3$ M^{-1} s^{-1} when the enzyme is preincubated with 0.10 mM N3ThDP (Figure 2B). The association of ThDP with the enzyme in the presence of substrate is complicated by the formation of intermediates (e.g., HEThDP) which increase the apparent affinity of the enzyme for the cofactor (*31*, *32*). However, the inhibition of the pre-steady-state process implies that the ThDP site is at least half-occupied by 0.10 mM N3ThDP.

Enzymatic Properties of Glu47 Mutants. Substitution of Glu47 with Gln or Ala yielded enzymes with measurable activities. The apparent affinity of the E47Q mutant for ThDP, as determined by the concentration for half-saturation of activity ($K_{0.5}$), is not significantly lower than that of the wild-type. The E47A mutant, on the other hand, shows a

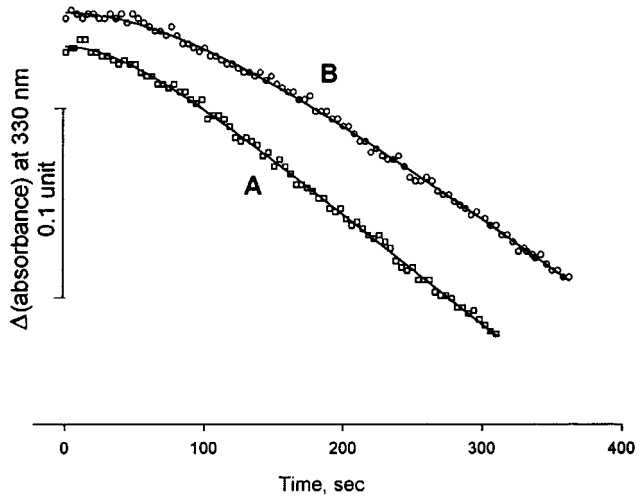

FIGURE 2: Inhibition by the analogue N3ThDP of AHAS activation on addition of ThDP. Wild-type AHAS II was preincubated at 37 °C in a cuvette containing 20 mM pyruvate, 10 mM $MgCl_2$, and 75 μM FAD in 0.1 M potassium phosphate buffer, pH 7.6, without (A) or with (B) 0.1 mM N3ThDP. At time 0, 2 μM ThDP was added to the cuvette. The disappearance of the absorbance of pyruvate at 330 nm was followed. The plots are offset for clarity. The lines are fits to the equation: $OD = y_0 + (v/b)e^{-bt} - vt$. The estimated values of b are 2.1×10^{-2} and 9.6×10^{-3} s^{-1}, for (A) and (B), respectively, with a standard error estimation of about 6%.

Table 2: Kinetic Parameters for Wild-Type AHAS II and Mutants at Glu47[a]

	wild-type	E47Q	E47A
specific activity (U mg^{-1})	20	2.0	1.6
relative activity (%)	≡100	10	8
K_m for pyruvate (mM)	5.0 ± 0.5	7.3 ± 1.1	7.7 ± 0.5
$k_{cat}/K_{m(pyr)}$ at pH 6.4 (M^{-1} s^{-1})[b]	2.4×10^3	22	6
$K_{0.5}$ for ThDP (μM)	0.65 ± 0.03	1.3 ± 0.1	29 ± 5
$K_{0.5}$ for FAD (μM)[c]	0.17 ± 0.04	0.14 ± 0.04	33 ± 6
specificity for 2KB (R)[d]	57 ± 7	48 ± 6	6.0 ± 1.3
K_i for SMM (μM)	0.80 ± 0.06	0.3 ± 0.1	0.6 ± 0.02

[a] The kinetic parameters were determined as described under Materials and Methods at 37 °C and pH 7.6. The buffer used was 0.1 M potassium phosphate containing 100 mM sodium pyruvate, 500 μM ThDP, 200 μM FAD, and 10 mM $MgCl_2$. The specific activities given here are accurate within 10−15%. [b] k_{cat}/K_m was determined at pH 6.4 under conditions similar to those described above, except for the use of Mops buffer. [c] The enzyme was stripped of endogenous FAD as described under Materials and Methods before determination of the half-saturating FAD concentration. [d] The specificity for 2-ketobutyrate as second substrate, R, is defined by: $R = (V_{AHB}/V_{AL})([\text{pyruvate}]/[2KB])$, where [2KB] is the concentration of 2-ketobutyrate and V_{AHB}/V_{AL} is the relative rate of formation of acetohydroxybutyrate and acetolactate, measured simultaneously in a competition experiment with 2-ketobutyrate and pyruvate (*20*), in the standard buffer.

significant decrease in affinity for ThDP, with $K_{0.5}$ 50-fold higher than the wild-type (Table 2). The specific activities of the purified E47Q and E47A mutants, in the presence of saturating concentrations of substrate and all cofactors (Table 2), were about 10% and 8% that of the wild-type activity, respectively. In both mutants, the K_m for pyruvate shows little change (Table 2). However, the mutations lead to a significant change in the pH dependence of the activity (not shown). For the wild-type enzyme, k_{cat}/K_m is maximal (4×10^3 M^{-1} s^{-1}) at pH 7.2−7.6, with an apparent pK of about 6.3 on the acidic side. This is shifted to higher pH by 0.5 and 1 unit, respectively, in the mutants E47Q and E47A. Thus, below pH 6.5, k_{cat}/K_m is about 1% that of the wild-type for E47Q and less than 0.5% that of wild-type for E47A (Table 2).

Table 3: Parameters for Proton Exchange at C2 of ThDP and for Acetolactate Synthesis

sample	proton exchange rate (s^{-1})[a]	k_{cat} for synthesis of acetolactate (s^{-1})[b]
AHAS II wild-type	332	23
E47Q	8	2.3
E47A	5.7	1.8
free ThDP	0.14	

[a] Rate constants for deprotonation of C2 in enzyme-bound and free ThDP were determined in 0.1 M potassium phosphate buffer at pH 7.6 and 37 °C by the ^{1}H NMR method (*13*) as described under Materials and Methods. [b] k_{cat} for the acetolactate synthesis reaction under standard conditions (see Materials and Methods) is calculated per active site, assuming two sites per holoenzyme and a protein molecular mass of 138 kDa.

Mutant E47Q is otherwise like the wild-type enzyme, while E47A shows very significant changes in several additional parameters (Table 2). E47A has a significantly lower affinity for FAD. It also shows a decrease in the substrate specificity parameter (R), which characterizes the preference of an AHAS for 2-ketobutyrate as second substrate and is determined in direct competition experiments (*20*).

Kinetics of H/D Exchange at the C2 Position of ThDP Bound to AHAS II. The rate of deprotonation of the enzyme bound-ThDP was measured by ^{1}H NMR analysis of the disappearance of the C2 proton after exchange with D_2O in quenched-flow experiments (*13*) (Table 3). The observed ThDP deprotonation rate in wild-type AHAS II is 332 s^{-1} under standard conditions at 37 °C, which is in the range reported for other enzymes at 4 °C (*12*, *13*, *33*, *34*). This rate is more than 3 orders of magnitude greater than the rate determined for the free cofactor under the same conditions, and is of course higher than the AHAS II synthase reaction, as expected (Table 3).

The ThDP proton exchange rates of the enzymes mutated at position E47 are 2 orders of magnitude slower than for the wild-type (Table 3), which suggests that glutamate is indeed involved in the deprotonation. For both mutants, the observed deprotonation rates are higher than the turnover rate, and thus are not rate-limiting in the synthesis of acetolactate by these mutant enzymes.

Nonlinear Dependence of AHAS Activity on Protein Concentration in the E47A Mutant. The activity of wild-type AHAS isozyme II shows a linear dependence on the concentration of the protein and a constant specific activity, even at very low enzyme concentrations (Figure 3). This is in contrast to the nonlinear behavior observed for isozyme III (*35*), and implies that the subunits of AHAS II are tightly associated. However, in the case of the E47 mutants, nonlinear behavior was observed and the apparent specific activity of the enzyme increases with protein concentration until it reaches a plateau (Figure 3). This behavior can be explained by an increased dissociation of the subunits of the mutant compared to the wild-type at low concentrations of the protein.

Mg^{2+}-Binding Site. Substitution of Asp428 by Asn or Glu yielded enzymes with measurable activities: 2.9 and 1.2 U mg^{-1} for D428N and D428E, respectively. As expected, the apparent affinities for Mg^{2+} of both D428 mutants decreased

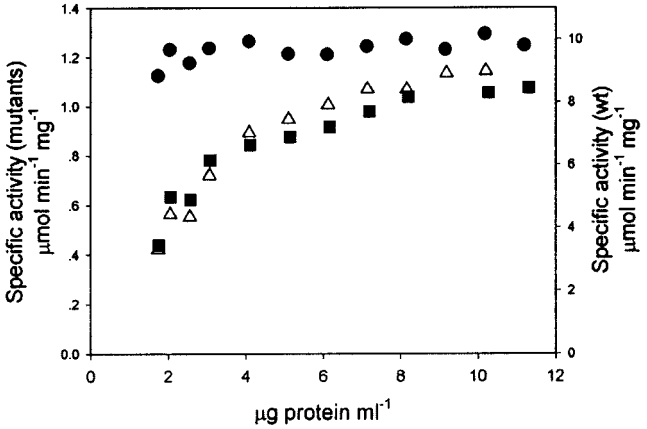

FIGURE 3: Protein concentration dependence of the specific activity of AHAS II wild-type and E47 mutants. The activity of wild-type (●) and E47Q (■) was measured as described under Materials and Methods in the presence of 100 μM ThDP, while that of E47A (△) was measured at 500 μM ThDP. The reaction times for the wild-type and the mutants were 4 and 40 min, respectively.

Table 4: Kinetic Parameters for Wild-Type AHAS II and Mutants at Asp428[a]

	wild-type	D428N	D428E
specific activity (U mg^{-1})	20	2.9	1.2
relative activity (%)	≡100	15.5	6
K_m for pyruvate (mM)	6.6 ± 0.5	7 ± 2	36 ± 3
$K_{0.5}$ for ThDP (μM)	1.9 ± 0.2	0.6 ± 0.2	192 ± 10
$K_{0.5}$ for Mg^{2+} (μM)[b]	10 ± 2	210 ± 20	360 ± 10
specificity for 2KB (*R*)[c]	57 ± 7	39 ± 8	43 ± 11
K_i for SMM (μM)	(0.80)[e]	3.2 ± 0.5	6 ± 1
K_m for K^+ (mM)[d]	ind	19 ± 10	35 ± 6

[a] The kinetic parameters were determined as described under Materials and Methods at 37 °C and pH 8.0. The buffer used was 0.1 M Tricine-KOH containing 80 mM sodium pyruvate, 500 μM ThDP, 100 μM FAD, and 10 mM $MgCl_2$, except that 100 mM pyruvate was used for mutant D428E. The specific activities given here are accurate within 10−15%. [b] For determination of the concentration of Mg^{2+} for half-activation of the enzyme, Mg^{2+} was first stripped from the protein samples as described under Materials and Methods, and the final free Mg^{2+} concentrations buffered with EDTA. [c] The specificity for 2-ketobutyrate as second substrate, *R*, is defined in footnote *c* of Table 2. [d] K^+ dependence was determined in 0.1 M Tricine-NaOH buffer, with increasing amounts of KCl. ind: rate is independent of K^+ concentration. [e] Inhibition of the wild-type enzyme by SMM was not determined separately in this buffer; the value given here is from Table 2.

significantly compared to the wild-type (Table 4). The K_m for Mg^{2+} increased from 10 μM to 210 and 360 μM for D428N and D428E, respectively.

In the presence of saturating Mg^{2+}, D428N shows little change in the apparent affinities for ThDP and pyruvate, or in pH dependence. The D428E mutant, on the other hand, shows significant decreases in affinity for ThDP and pyruvate, even when the enzyme is saturated with all other cofactors (Table 4). Both mutants show preferences for 2-ketobutyrate as second substrate (*R*) that are similar to wild-type (Table 4).

When initial experiments were carried out to determine the Mg^{2+} affinity of the mutants at D428 in a Tricine-NaOH buffer, their activities were found to be surprisingly low compared to those in a potassium phosphate buffer. The wild-type enzyme, on the other hand, showed very similar activities in the two buffers. An examination of the KCl dependence of these enzymes in a Tricine-NaOH buffer (Figure 4) revealed that while the wild-type shows no

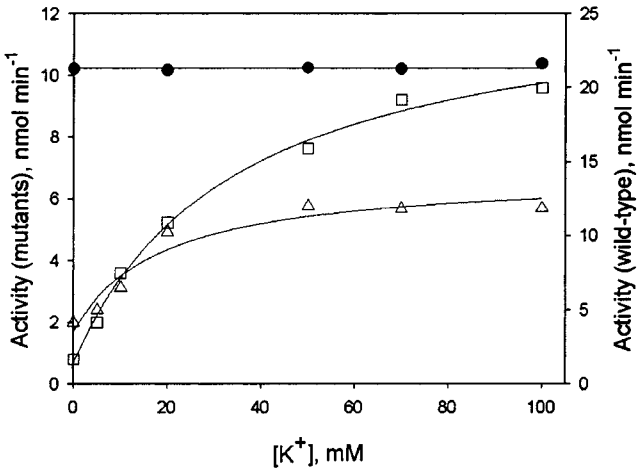

FIGURE 4: K^+ dependence of the activity of wild-type AHAS II (●) and mutants D428N (△) and D428E (□). The concentration of wild-type protein was 0.8 μg/mL, and that of each of the mutants was 5 μg/mL. The activity was measured as described under Materials and Methods, in Tricine-NaOH buffer with varying amounts of KCl.

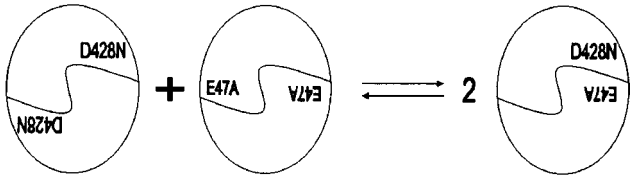

FIGURE 5: Schematic illustration of a possible complementation equilibrium in AHAS. Catalytic subunits exchange between enzymes with mutations in different domains, to yield the hybrid enzyme on the right which has one doubly defective active site and one normal active site.

potassium dependence, the activities of mutants D428N and D428E were stimulated 2.5- and 10-fold by potassium, respectively. Their apparent K^+ affinities were 19 and 35 mM, respectively.

Complementation between D428N and E47A. Our model for AHAS assumes that residues D428 and E47 in a single active site are contributed by different polypeptides (Figure 1). If mutated enzymes easily dissociate to release monomers of catalytic subunits and can then reassociate, some of the reassembled protein molecules in a mixture of mutants at these positions might be hybrids containing one "normal" active site and one site mutated at both positions (Figure 5). This prediction was tested in an experiment in which the E47A and D428N mutants were preincubated together in different ratios for 20 min at 37 °C. Conditions for measurement of the activity (20 μM ThDP, 40 mM pyruvate, 75 μM FAD, 100 μM $MgCl_2$ in a 0.1 M potassium phosphate buffer, pH 7.6) were chosen so that neither mutant alone showed high activity (see Tables 2 and 4). As seen in Figure 6, mixtures gave significantly higher activity than the sum of the activities of the parent mutants. The highest activity was obtained when the ratio between the mutants was near 1:1.

DISCUSSION

The properties of the mutant proteins studied here support the homology model for a dimer of catalytic subunits of AHAS II (*17*), which was based on the structure of *Lp*POX. In this model, the essential cofactor ThDP is bound

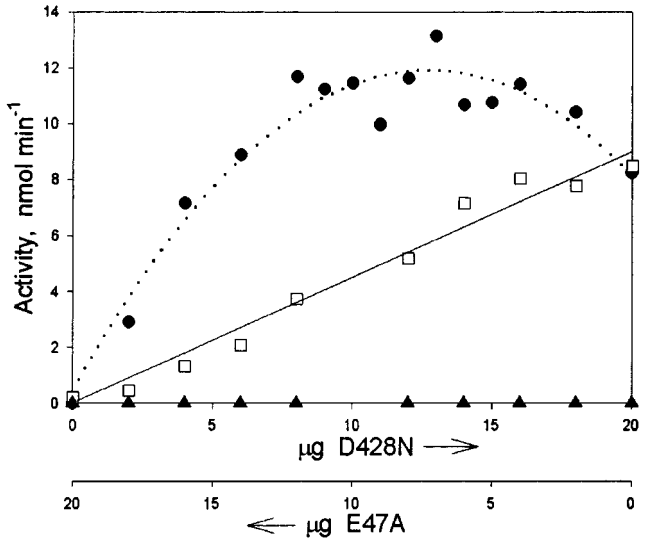

FIGURE 6: Complementation between mutants E47A and D428N. The activity of varying amounts of D428N (□) and E47A (▲) was determined in a 0.1 M potassium phosphate buffer, pH 7.6 at 37 °C, in the presence of 20 μM ThDP, 40 mM pyruvate, 75 μM FAD, and 100 μM $MgCl_2$, suboptimal concentrations of these factors for both mutants (see Table 2). The activity of mixtures of the two mutants in different ratios (●), containing 20 μg of total protein, was determined after preincubation of the mixtures at 37 °C for 20 min. The upper abscissa shows the amounts of D428N increasing from left to right and the lower that of E47A, increasing from right to left.

in a specific conformation at the interface between catalytic subunits, with one subunit providing contacts with the diphosphate moiety and the other with the aminopyrimidine (Figure 1).

The essential divalent metal cation is ligated to one oxygen of each of the ThDP phosphate groups, as well as to side chain oxygen atoms of Asp428 and Asn455 and to a backbone carbonyl (Figure 1). These interactions are highly conserved in a variety of ThDP-dependent enzymes (*1*, *2*, *5*−*9*) and are assumed to play a major role in anchoring ThDP in the active site. When the activity of the protein is measured as a function of Mg^{2+} concentration, in the presence of saturating concentrations of the substrate and of the other cofactors including ThDP, the concentration for half-saturation ($K_{0.5}$) is effectively a measure of the affinity of the enzyme−ThDP complex for the metal ion. Replacement of the carboxylate of Asp428 with a carboxamido group, in D428N, leads to a 20-fold decrease in that affinity (Table 4). On the other hand, $K_{0.5}$ for ThDP in the presence of a saturating Mg^{2+} concentration measures the apparent kinetic affinity of the enzyme−Mg^{2+} binary complex for this cofactor. One would not expect that affinity to be decreased in the D428N mutant, which should have a very similar active-site geometry and a more positive net charge on the metal. The measured apparent ThDP affinity and also other properties of this mutant enzyme are very much like those of the wild-type (Table 4), although its activity is lower.

The replacement of Asp428 by glutamate (D428E), on the other hand, has less straightforward effects on the protein, presumably because the longer side chain is incompatible with the required local geometry of the complex. The apparent affinity of the mutant enzyme−ThDP complex for Mg^{2+} is 36-fold lower than that of the wild-type, despite conservation of the charged group, while the apparent affinity of the enzyme−Mg^{2+} complex for ThDP is decreased nearly 300-fold.

The role of a conserved aspartate in the thiamin diphosphate motif, which is directly involved in Mg^{2+} binding, has only been examined experimentally in a few cases. In pyruvate decarboxylase from *Zymomonas mobilis*, replacement of the Mg^{2+} ligand Asp440 by glutamate also leads to an enzyme with a decreased affinity for both Mg^{2+} and ThDP, and low but significant activity (*36*). Surprisingly, replacement of the same amino acid by Asn seems to completely abolish activity and ThDP binding (*37*). The decarboxylase (E1α) component of the human mitochondrial branched-chain ketoacid dehydrogenase has glutamate as the acidic ligand to magnesium rather than aspartate; its mutation is reported to lead to a completely inactive enzyme when tested with normal Mg^{2+} concentrations (*38*). Before the structure of any ThDP-dependent protein was known, the ThDP-binding motif G(D/E)GX_{24-27}NN had been recognized on the basis of sequence similarities (*9*). Its functional significance was first tested by mutagenesis of the second glycine in the motif in the E1 component of *E. coli* pyruvate dehydrogenase (*39*). The decarboxylase activity of E1-G231 mutants was reduced by an order of magnitude, while the overall pyruvate dehydrogenase activity was reduced by 3−4 orders of magnitude (*39*, *40*). This system shows complex time-dependent activation by ThDP and pyruvate, with which a G231A or G231S mutation seems to intefere (*40*).

In all the ThDP-dependent enzymes which have been examined, there is a conserved glutamate residue within hydrogen-bonding distance of N1′ of the aminopyrimidine moiety. This interaction is involved both in binding of the cofactor and in its activation (*13*). The relatively conservative replacement of Glu47 in AHAS II, by glutamine, led to an active protein, most of whose properties were similar to those of the wild-type (Table 2). The affinity of this variant for ThDP is only decreased 2-fold. The less conservative replacement of this glutamate by alanine (E47A) also leads to an active protein, although this protein shows a 50-fold reduction in affinity for ThDP and other changes in properties discussed below. The activities of these mutants at pH 7.6, near optimum for the wild-type protein, about 10% and 8% of that of the wild-type, respectively, do not (at first consideration) appear to be consistent with an essential role for the residue in activation of ThDP. The homologous Glu → Gln mutants in transketolase (*11*), yeast pyruvate decarboxylase (*14*), *Z. mobilis* pyruvate decarboxylase (*41*), and human pyruvate dehydrogenase (*42*) have 2, 0.04, 0.5, and 5%, respectively, of the specific activity of the wild-type enzymes. The pyruvate dehydrogenase mutant also showed a 50-fold increase in K_S for ThDP (*42*), similar to the change we observed. A recently reported Glu → Ala mutant in mitochondrial branched-chain ketoacid dehydrogenase has no detectable activity (*38*).

Examination of the rate of exchange of the C2 proton of bound ThDP in the AHAS II E47 mutants shows that the glutamate−ThDP N1′ interaction has a significant effect on the rate of ionization of the cofactor. The exchange rate in E47Q is 40 times lower than that observed with the wild-type protein, 8 s^{-1} at 37 °C, and is close to rate-limiting for turnover in this mutant (Table 3). The proton exchange rate in wild-type AHAS II is far from rate-limiting; this could certainly be the reason for the moderate effect of mutation

on the overall synthase activity. The E47A mutant has a somewhat lower rate of exchange and lower turnover rate than the conservative mutant E47Q (Table 3). These results are comparable to those observed with mutants of other ThDP-dependent enzymes altered at the homologous glutamate (*13*): Yeast pyruvate decarboxylase mutant E51Q has a ThDP C2 proton exchange rate of 1.7 s^{-1} at 4 °C (when activated by pyruvamide), as compared to >600 s^{-1} for the wild-type, and transketolase mutant E418A has a proton exchange rate of 0.4 s^{-1} at 4 °C, as compared to 61 s^{-1} for the wild-type.

We considered the possibility that there is an alternative mechanism for ionization of ThDP in AHAS, in which another group in the enzyme active site activates the pyrimidine C4′−N directly, or replaces it as the base which removes the thiazole C2 proton (see Figure 1). The very low activity observed when ThDP is replaced by N3ThDP (<0.5%) demonstrates that the N1′ nitrogen of the aminopyrimidine is required in AHAS, as it is in other ThDP-dependent enzymes (*10*). The significant but low proton exchange rate in, e.g., AHAS II E47Q suggests that even in the absence of the Glu47 carboxylate, the aminopyrimidine can play a role in deprotonation of the thiazole if it is held in an appropriate orientation in proximity to C2. The observed shift in the pH dependence of k_{cat}/K_m in the mutants at Glu47 could be interpreted as due to the loss of the contribution of the ionization of the side chain of this residue to the activity of the protein. It might, of course, reflect an increase in the apparent pK_a of some other group involved in the overall reaction. A study of the pH dependence of individual steps in the overall reaction will be required to clarify this point.

In some ThDP-dependent enzymes, the aminopyrimidine may have additional functions. For example, in the decarboxylases it may also be involved in deprotonation of the α-hydroxyl group of HEThDP (*34*). Such a function is possibly unimportant in, e.g., transketolase or AHAS.

All ThDP-dependent enzymes whose crystal structures have been determined have conserved binding interactions with the cofactor. Mutagenesis of AHAS II supports the notion that these interactions are conserved in AHAS and supports our identification of some of these homologous residues. The effective complementation of the E47A and D428N mutants, when examined in the presence of cofactor concentrations far below saturation for either mutant alone (Figure 6), shows that each ThDP site in the holoenzyme is derived from two different polypeptides (see Figure 5) and that in the case of these mutants dissociation and reassociation of the holoenzyme is significant on the time scale of the experiment.

Because ThDP is bound at the catalytic subunit interface, one expects there to be a reciprocal relationship between assembly of the quaternary structure and cofactor binding. In small-angle X-ray scattering experiments, König has observed that the oligomerization of *Lp*POX is dependent on the presence of ThDP (S. König, personal communication). AHAS II mutants E47Q and E47A, in which one of the ThDP-anchoring groups is altered, show dependence of the specific activity on the protein concentration (Figure 3), which is indicative of concentration-dependent assembly of the holoenzyme. From this behavior, one can estimate for either mutant enzyme that only about half of the protein is fully assembled at a protein concentration of 2×10^{-8} M. The holoenzyme of the wild-type protein is apparently stable enough so that no evidence for the concentration dependence of its specific activity is seen under the conditions of our experiments. Direct examination of the oligomerization state of these and other AHAS mutants would be of interest.

The biosynthetic activity of AHAS obviously involves many other factors beyond the binding and deprotonation of ThDP; if it did not, the enzyme would be expected to have the same activities as, e.g., *Lp*POX. Some of the properties of the mutations described here are very interesting in this regard. We have identified a region of the active site of AHAS II, including Trp464, as critical to the high specificity of this enzyme for recognition of 2-ketobutyrate as second substrate and formation of acetohydroxybutyrate (*17*). The E47A mutant has a significantly decreased specificity for 2-ketobutyrate ($R = 6$, see Table 2), even though Glu47 is far from the plausible recognition site. One possible explanation for this is that the position of the bound ThDP in the active site of this mutant, in which a number of atoms of a side chain in contact with the cofactor have been removed, is shifted sufficiently to alter the interaction between the enzyme and its substrates. The decrease in the affinity of this mutant for FAD by more than 2 orders of magnitude might also be caused by a local loosening of the protein structure.

One additional, somewhat surprising observation is the potassium dependence seen in D428N and D428E, but not in the wild-type AHAS II (Figure 4). Unlike AHAS II, the wild-type AHAS III shows a weak but real dependence on monovalent cations (*43*). The absence of K^+ dependence in wild-type AHAS II suggests either that occupation of the monovalent cation sites in this protein by, e.g., Na^+ is sufficient to stabilize the required active structure, or that one or more K^+ ions are held so firmly in the wild-type enzyme that they are not lost during protein purification. A cation site, tentatively identified as a site for Na^+, has been observed on a diad axis in the monomer−monomer interface of *L*pPOX (*44*), and involves ligands from Met452 and Gln455 of both subunits. These amino acids are part of the ThDP motif and are conserved in AHASs (Met433 and Gln436 in AHAS II) and close to Asp428, whose mutation leads to K^+ dependence. We are investigating whether a monovalent cation site at this position affects assembly of an AHAS holoenzyme.

ACKNOWLEDGMENT

We are grateful to Hagay Shmuely and Monika Einav for their contributions to the construction and testing of the pRGM plasmid.

REFERENCES

1. Lindqvist, Y., Schneider, G., Ermler, U., and Sundstrom, M. (1992) *EMBO J. 11*, 2373−2379.
2. Muller, Y. A., Lindqvist, Y., Furey, W., Schulz, G. E., Jordan, F., and Schneider, G. (1993) *Structure 1*, 95−103.
3. Dyda, F., Furey, W., Swaminathan, S., Sax, M., Farrenkopf, B., and Jordan, F. (1993) *Biochemistry 32*, 6165−6170.
4. Muller, Y. A., and Schulz, G. E. (1993) *Science 259*, 965−967.
5. Dobritzsch, D., König, S., Schneider, G., and Lu, G. (1998) *J. Biol. Chem. 273*, 20196−20204.

6. Hasson, M. S., Muscate, A., McLeish, M. J., Polovnikova, L. S., Gerlt, J. A., Kenyon, G. L., Petsko, G. A., and Ringe, D. (1998) *Biochemistry 37*, 9918−9930.
7. Aevarsson, A., Seger, K., Turley, S., Sokatch, J. R., and Hol, W. G. J. (1999) *Nat. Struct. Biol. 6*, 785.
8. Chabriere, E., Charon, M. H., Volbeda, A., Pieulle, L., Hatchikian, E. C., and Fontecilla Camps, J.-C. (1999) *Nat. Struct. Biol. 6*, 182−190.
9. Hawkins, C. F., Borges, A., and Perham, R. N. (1989) *FEBS Lett. 255*, 77−82.
10. Golbik, R., Neef, H., Hübner, G., König, S., Seliger, B., Meshalkina, L., Kochetov, G. A., and Schellenberger, A. (1991) *Bioorg. Chem. 19*, 10−17.
11. Wikner, C., Meshalkina, L., Nilsson, U., Nikkola, M., Lindqvist, Y., Sundstrom, M., and Schneider, G. (1994) *J. Biol. Chem. 269*, 32144−32150.
12. Hübner, G., Tittmann, K., Killenberg-Jabs, M., Schaeffner, J., Spinka, M., Neef, H., Kern, D., Kern, G., Schneider, G., Wikner, C., and Ghisla, S. (1998) *Biochim. Biophys. Acta 1385*, 221−228.
13. Kern, D., Kern, G., Neef, H., Tittmann, K., Killenberg Jabs, M., Wikner, C., Schneider, G., and Hübner, G. (1997) *Science 275*, 67−70.
14. Killenberg-Jabs, M., König, S., Eberhardt, I., Hohmann, S., and Hübner, G. (1997) *Biochemistry 36*, 1900−1905.
15. Nilsson, U., Lindqvist, Y., Kluger, R., and Schneider, G. (1993) *FEBS Lett. 326*, 145−148.
16. Green, J. B. (1989) *FEBS Lett. 246*, 1−5.
17. Ibdah, M., Bar-Ilan, A., Livnah, O., Schloss, J. V., Barak, Z., and Chipman, D. M. (1996) *Biochemistry 35*, 16282−16291.
18. Ott, K.-H., Kwagh, J.-G., Stockton, G. W., Sidorov, V., and Kakefuda, G. (1996) *J. Mol. Biol. 263*, 359−368.
19. Umbarger, H. E. (1987) in *Escherichia coli and Salmonella typhimurium. Cellular and molecular biology* (Neidhardt, F. C., Ingraham, J. L., Low, B. L., Magasanik, B., Schaechter, M., and Umbarger, H. E., Eds.) pp 352−367, American Society for Microbiology, Washington, DC.
20. Gollop, N., Damri, B., Barak, Z., and Chipman, D. M. (1989) *Biochemistry 28*, 6310−6317.
21. Schellenberger, A. (1967) *Angew. Chem., Int. Ed. Engl. 6*, 1024−1035.
22. Lawther, R. P., Calhoun, D. H., Adams, C. W., Hauser, C. A., Gray, J., and Hatfield, G. W. (1981) *Proc. Natl. Acad. Sci. U.S.A. 78*, 922−925.
23. Hill, C. M., Pang, S. S., and Duggleby, R. G. (1997) *Biochem. J. 327*, 891−898.
24. Sambrook, J., Fritsch, E. F., and Maniatis, T. (1989) *Molecular cloning: a laboratory manual*, Cold Spring Harbor Laboratories, Cold Spring Harbor, NY.
25. Ho, S. N., Hunt, H. D., Horton, R. M., Pullen, J. K., and Pease, L. R. (1989) *Gene 77*, 51−59.
26. Schloss, J. V., VanDyk, D. E., Vasta, J. F., and Kutny, R. M. (1985) *Biochemistry 24*, 4952−4959.
27. Epelbaum, S., Chipman, D. M., and Barak, Z. (1990) *Anal. Biochem. 191*, 96−99.
28. Barak, Z., Chipman, D. M., and Gollop, N. (1987) *J. Bacteriol. 169*, 3750−3756.
29. Bradford, M. (1976) *Anal. Biochem. 72*, 248−254.
30. Martell, A. E., and Smith, R. M. (1974) *Critical Stability Constants*, Plenum Press, New York.
31. Hennig, J., Kern, G., Neef, H., Spinka, M., Bisswanger, H., and Hubner, G. (1997) *Biochemistry 36*, 15772−15779.
32. Schloss, J. V., and Aulabaugh, A. (1990) in *Biosynthesis of Branched Chain Amino Acids* (Barak, Z., Chipman, D. M., and Schloss, J. V., Eds.) pp 329−356, VCH, Weinheim, Germany.
33. Tittmann, K., Proske, D., Spinka, M., Ghisla, S., Rudolph, R., Hübner, G., and Kern, G. (1998) *J. Biol. Chem. 273*, 12929−12934.
34. Tittmann, K., Mesch, K., Pohl, M., and Hübner, G. (1998) *FEBS Lett. 441*, 404−406.
35. Sella, C., Weinstock, O., Barak, Z., and Chipman, D. M. (1993) *J. Bacteriol. 175*, 5339−5343.
36. Candy, J. M., and Duggleby, R. G. (1994) *Biochem. J. 300*, 7−13.
37. Diefenbach, R. J., Candy, J. M., Mattick, J. S., and Duggleby, R. G. (1992) *FEBS Lett. 296*, 95−98.
38. Wynn, R. M., Ho, R., Chuang, J. L., and Chuang, D. T. (2001) *J. Biol. Chem. 276*, 4168−4174.
39. Russell, G. C., Machado, R. S., and Guest, J. R. (1992) *Biochem. J. 287*, 611−619.
40. Yi, J. Z., Nemeria, N., McNally, A., Jordan, F., Machado, R. S., and Guest, J. R. (1996) *J. Biol. Chem. 271*, 33192−33200.
41. Candy, J. M., Koga, J., Nixon, P. F., and Duggleby, R. G. (1996) *Biochem. J. 315*, 745−751.
42. Fang, R., Nixon Peter, F., and Duggleby Ronald, G. (1998) *FEBS Lett. 437*, 273−277.
43. Vyazmensky, M., Sella, C., Barak, Z., and Chipman, D. M. (1996) *Biochemistry 35*, 10339−10346.
44. Muller, Y. A., Schumacher, G., Rudolph, R., and Schulz, G. E. (1994) *J. Mol. Biol. 237*, 315−335.

BI0104524